

Trimethylamine as a Probe Molecule To Differentiate Acid Sites in Y–FAU Zeolite: FTIR Study

Francisca Romero Sarria, Vanessa Blasin-Aubé, Jacques Saussey, Olivier Marie,* and Marco Daturi

Laboratoire Catalyse & Spectrochimie, CNRS-ENSICAEN, 6 Bd du Maréchal Juin, 14050 Caen Cedex, France

Received: March 20, 2006; In Final Form: May 5, 2006

In heterogeneous catalysis acidity has a very important influence on activity and selectivity: correct determination of acidic properties is a base to improve industrial processes. The aim of this work was to study trimethylamine (TMA) as a probe molecule able to distinguish between the different Brønsted acid sites in zeolitic frameworks. Our work mainly focused on faujasite-type zeolites because the HY zeolite is one of the most used acidic catalysts in industrial processes. In this paper, typical IR bands assigned to TMA-protonated species (formed in supercages) are detected in the HY zeolite. TMA interacting by hydrogen bonding with the acid sites located in the sodalite units is also observed. The wavenumbers of some typical IR bands assigned to TMA-protonated species appear to depend on the acidic strength, and a complementary study with ZSM-5 and X-FAU samples confirms this proposition.

Introduction

Zeolite compounds have extensive application in different fields as adsorbents, traditional ion exchange, and catalysts. Their use as catalysts is especially important in the petroleum refining industry, where these compounds find applications in processes of fluid catalytic cracking, hydrocracking, aliphatic alkylation, isomerization, etc. In particular, the HY zeolite has been extensively used in this type of process since 1962. Most applications are related to both the acidic properties and the shape-selective behavior of aluminosilicates.¹ These microporous compounds have the majority of their active sites inside their structure, and molecules have to diffuse through the structure to react.² Therefore, the channel size as well as the relative abundance of acid sites into the different cavities become the fundamental parameters to improve reactions needing acidic catalysis.

According to Datka et al.,³ the acid properties in zeolite compounds depend on chemical and geometric factors. The chemical factor concerns the number of next neighboring Al for a given Si–OH–Al group, while the geometric factor takes into account the distances and angles formed between Al, Si, and O atoms. For a non-dealuminated Y zeolite, the chemical factor seems to be the most influential parameter. A great number of works using different techniques have been devoted to investigating the acidic properties of zeolites. Among the common techniques, basic probes adsorption followed by IR spectroscopy^{4–6} and NH₃-TPD^{7–9} are widely used.

The results obtained from probe molecules adsorption are sometimes complex because of the heterogeneity of the probed sites (chemical and geometric factors); moreover, the number of Brønsted acid sites determined in this way is generally fewer than that expected from the Si/Al ratio.¹⁰ The pyridine molecule is commonly used as a basic probe to characterize acidic sites. However, exact determination of the acidic strength using this molecule requires a complex study of the IR spectra in the ν -

(NH) region.¹¹ Low-temperature CO adsorption in zeolites is interesting to obtain acidic strength,¹² but it often leads to the disappearance of the hydroxyls, so it is hardly possible to discriminate an interaction with one single acidic site. The combined adsorption of pyridine and CO has been used to obtain information about the accessibility of sites⁶ inside mordenite, but for the study of the FAU-type zeolite, CO was revealed to be useless because of the very small interaction taking place with constrained hydroxyls.¹³

The ammonia TPD technique is based on the desorption temperature of the previously adsorbed NH₃ in the acidic zeolite, relating higher temperatures with more acidic sites and lower temperatures with less acidic sites (Brønsted and Lewis). However, it is known that ammonium ions formed in a three-dimensional structure (free from Lewis sites) give rise to formation of various species differently coordinated with the basic oxygen atoms forming the zeolitic walls (monodentate, bidentate, tridentate, and tetradentate species).¹⁴ Formation of each of these species depends on both acid strength and confinement effect (chemical and geometric factors³). Thus, it is possible to conceive the presence of sites having the same number of next-nearest Al neighbors but located in structures with different cavity sizes. Obviously, a NH₃ molecule will coordinate in a different way in such equivalent clusters. Considering that in a smaller cavity formation of ammonium with a higher coordination is easier, the response of NH₃-TPD for this kind of species will not be proportional to the real acidic strength of the site since species with higher coordination are supposed to desorb at higher temperature. Therefore, a kind of “false acidic strength ranking” can be estimated by the NH₃-TPD method. On the contrary, we propose (for a given chemical factor) that the NH₃-desorption temperatures are related to coordination of the formed ammonium species in a zeolitic structure. This fact may explain why Maache et al.⁶ found contradictory results for the acidity of H-mordenite from NH₃-TPD and CO adsorption experiments.

Thus, it may be interesting to develop the use of a probe molecule able to differentiate the acid sites located in different

* To whom correspondence should be addressed. E-mail: olivier.marie@ensicaen.fr.

cavities of a HY sample that is also acidic strength sensitive for sites located in the large cavities (chemical factor). Adsorption of probe molecules with increasing sizes (so a limited access to zeolitic cavities due to their steric hindrance) has been used to determine the localization of acid sites in the framework¹⁵ or the external acidity in some types of mesoporous materials,¹⁶ but the comparison of acid strength was not straightforward.

In previous work it was shown that trimethylamine (TMA) adsorption at room temperature leads to interaction with hydroxyl groups located in large cavities and sodalite units of a HY zeolite, while the hydroxyl groups located in the prisms are not interacting with this probe molecule.¹⁷ Also, taking into account some solid-state NMR data,¹⁸ TMA adsorption gives rise to trimethylammonium ion formation in the supercages, but it is not able to enter inside the sodalite units whose protons are proposed to only interact by hydrogen bonding. We will confirm that the interaction between TMA and zeolitic hydroxyls depends on the position of OH groups (supercages or sodalite units), and we will observe these different interactions by IR spectroscopy. Furthermore, we must stress that the very low acidity of the TMA hydrogen atoms (methyl groups) prevents them from interacting with the zeolitic basic oxygen, which is the main problem in the case of ammonia adsorption.

Experimental Section

The infrared spectra were recorded at room temperature with a Nicolet Magna 550 FTIR spectrometer with a MCT detector using an optical resolution of 2 cm⁻¹ and a one level zero-filling treatment for spectrum display. These conditions ensured 1 cm⁻¹ precision for sharp peaks such as the ones corresponding to $\nu(\text{CH})$ vibration modes. For “in situ” studies, the self-supported wafers of zeolites (2 cm², 7–10 mg) were placed in a quartz infrared cell and, prior to the adsorption experiments, carefully activated by heating under a vacuum for 10 h (1 K min⁻¹, 673 K, 10⁻³ Pa).

Trimethylamine (98% pure) was provided by Fluka. It was further purified by low-temperature trapping before use.

Four zeolite samples were used for this study: H–ZSM-5 (Si/Al = 29, H/Al = 1), HY (Si/Al = 2.72, H/Al = 1), NaHX40 (Si/Al = 1.21, H/Al = 0.4, and Na/Al = 0.6), and NaHX10 (Si/Al = 1.21, H/Al = 0.1, and Na/Al = 0.9). The last two were prepared from NaX (Linde) by partial ion exchange with a 0.25 M solution of NH₄Cl followed by washing with distilled water until chloride ions were no longer detected in the solution. The powders were then dried at 373 K before in situ experiments, where calcinations were conducted as described above. Si/Al and Na/Al ratios were obtained by atomic absorption, whereas the H/Al ratio was deduced from the absence of extraframework aluminum as observed by ²⁷Al MAS NMR.

The adsorptions were performed by successive introduction of well-known doses inside the infrared cell containing the previously activated wafer. After each dose of probe molecule, infrared spectra were recorded.

Results and Discussion

The methodology for characterizing sites on a material by probe molecule adsorption followed by FTIR requires a very good knowledge of both the vibrational modes of the molecule alone and the shift that they may undergo when the molecule interacts with a particular site.¹⁹ With the aim of obtaining the required information about the TMA behavior, careful study of IR spectra after TMA adsorption in H–ZSM-5, HY, and HNaX zeolites was carried out. First, study of the IR spectra obtained after TMA adsorption in a H–ZSM-5 zeolite (having channels

big enough to avoid accessibility problems) made possible assignment of typical IR bands to protonated species (trimethylammonium ion). Comparison of these spectra with those obtained after TMA adsorption in the HY zeolite (different accessibility and acidity) will evidence the presence of different types of interactions between the probe molecule and the hydroxyls. Furthermore, studying well-known less acidic NaHX samples⁵ will allow us to propose the wavenumber of the $\nu(\text{NH})$ vibration as a measure of the acidic strength. This study may be a complementary approach to develop a reliable method to characterize acidity in zeolite compounds.

TMA Adsorption on H–ZSM-5. Olson et al.,²⁰ studying the structural properties of H–ZSM-5 zeolite, established that a steric effect is detected when molecules with a diameter higher than 6.9 Å are adsorbed while mobility into the channels remains high for molecules with a diameter lower than 5.8 Å. The diameter of the TMA molecule is ~5.24 Å,²¹ and therefore, no problems from steric hindrance or low mobility are expected during the TMA adsorption in H–ZSM-5 zeolite. The spectra recorded after TMA adsorption at room temperature in the H–ZSM-5 sample are shown in Figure 1. The corresponding amounts of adsorbed TMA (from 80 to 980 $\mu\text{mol g}^{-1}$) are typical of coverage levels for which the interaction takes place predominantly with the acidic hydroxyls: SiOHAl leading to disappearance of the corresponding $\nu(\text{OH})$ band at 3610 cm⁻¹. For these adsorbed amounts, little interaction with silanols, SiOH (disappearing band at 3746 cm⁻¹), is observed, but the corresponding TMA vibration bands are small. Focusing on these TMA vibration modes (3200–2400 and 1600–1350 cm⁻¹) it is worth noting that no new bands and no wavenumber shifts are detected during adsorption of increasing quantities. This confirms the formation of one main type of species in this structure. According to Datka et al.,²² heterogeneity of OH groups in H–ZSM-5 is only detected for zeolites with Si/Al > 50. In our case (Si/Al = 29), we thus observe only one type of site as expected.

Detailed observation of Figure 1 enables us to distinguish three main IR regions for adsorbed TMA: 3200–3000, 3000–2400, and 1600–1350 cm⁻¹. We will discuss these vibrational ranges separately.

Region 3200–3000 cm⁻¹. Infrared bands in this region are absent for TMA in its liquid form; nevertheless, some data about their occurrence have already been reported in the literature. For example, Ouasri et al.,²³ studying the structure of trimethylammonium hexafluorosilicate (an ionic salt in which TMA is present in its protonated form), assigned the vibrations at 3050 and 2970 cm⁻¹ to $\nu_{\text{asym}}(\text{C–H})$ and $\nu_{\text{sym}}(\text{C–H})$ of the methyl groups, respectively. It is quite surprising to observe $\nu_{\text{sym}}(\text{C–H})$ at such a high wavenumber; however, both (CH) stretching vibrations are shifted toward higher wavenumbers upon interaction with a nitrogen lone pair as discussed below. Also, Harmon et al.,²⁴ studying different tetramethylammonium salts, observed that the $\nu(\text{C–H})$ modes have two components (symmetric and asymmetric) between 3200 and 2900 cm⁻¹. Bands at $\bar{\nu} > 3000$ cm⁻¹ were also observed by Taillander²⁵ in complexes of TMA with BF₃. In this case, the obtained values for the bands were slightly lower (3035 cm⁻¹ with a shoulder at 3011 cm⁻¹) than for the protonated species. According to a theoretical study of amines adsorption in HMOR to only form alkylammonium,²⁶ an increase in the C–H stretching wavenumbers of protonated species (compared with the gas phase) was obtained: 80–174 cm⁻¹ for Me₃NH⁺ species. The appearance of bands in this region is explained as follows: the nitrogen lone pair stabilizes the N–C bond by a hyperconjugation effect,²⁷ and when an

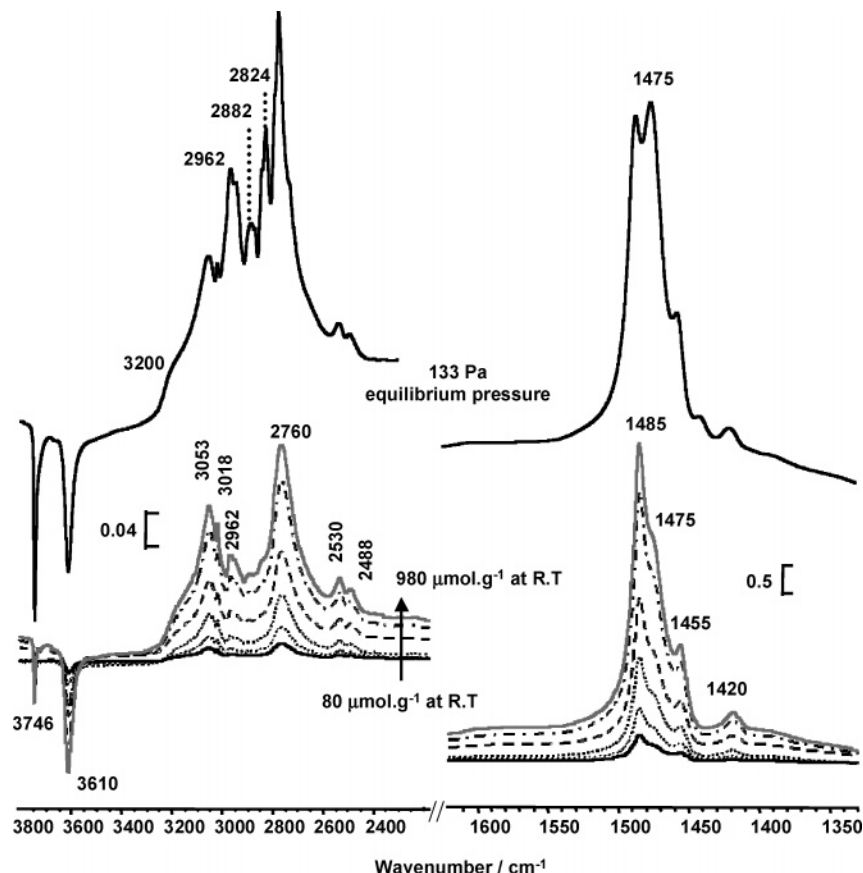


Figure 1. TMA adsorption at room temperature in a H-ZSM-5 (small increasing quantities).

interaction with another molecule involving the nitrogen lone pair occurs, both elongation of the CN bonds [decreasing $\nu(\text{C}-\text{N})$ wavenumber] and shortening of the CH bonds [increasing $\nu_{\text{asym}}(\text{C}-\text{H})$ and $\nu_{\text{sym}}(\text{C}-\text{H})$ wavenumbers] are observed.

On the other hand, adsorption of trimethylamine on Ge(100)-2 \times 1 surface was carried out by Collin et al.²⁸ These authors detected a molecular chemisorption by formation of a Ge-N dative bond. In this case, no bands in the 3200–3000 cm^{-1} region were observed and the stretching mode for the methyl groups appears between 3000 and 2700 cm^{-1} (lower values than previous compounds).

To resume the above literature data, one can conclude the formation of an interaction involving a transfer of the nitrogen lone pair (total or partial) increases the wavenumber of $\nu(\text{C}-\text{H})$ bands and the shift magnitude is a function of the interaction strength. Therefore, this region of the spectrum should be very interesting to obtain some data about the relative acidic strength of the coordination site.

In our case, the appearance of two bands in this region (3053 and 3018 cm^{-1} to which $\nu_{\text{asym}}(\text{C}-\text{H})$ of the methyl groups can be assigned) allows us to say that species showing a strong interaction are formed after TMA adsorption at room temperature. Since the wavenumbers typical of interacting TMA remain constant for increasing surface coverage and the bands are sharp, one can think that all the acid sites interacting with the probe molecule generate the same species. We would like to emphasize that the intensity of the $\nu(\text{CH})$ component below 3000 cm^{-1} (at 2962 cm^{-1}) is rather low and its relative intensity compared with that of the doublet at $\bar{\nu} > 3000 \text{ cm}^{-1}$ is kept low for low coverage levels. On the contrary, when weaker interactions with silanols became the majority (top spectrum of Figure 1: 133 Pa equilibrium pressure), sharp peaks below 3000 cm^{-1} became dominant with new components at 2882 and 2824 cm^{-1} , which

are typical of pseudo-liquid TMA. The broad and not very intense shoulder around 3200 cm^{-1} also seems to be related to the observed decrease of the silanols species (3746 cm^{-1}). This hypothesis was confirmed by the TPD experiments during which the disappearance of bands at $\sim 3200 \text{ cm}^{-1}$ was observed in parallel with the reappearance of the 3746 cm^{-1} band (figure not shown).

In summary, studying this region one can conclude that interaction between TMA probe molecule and strongly acidic hydroxyl groups of the H-ZSM-5 zeolite leads to a unique strongly bonded species, while a weaker interaction with the silanol groups is observed. It is necessary to remember that interactions between the methyl groups and the basic oxygens forming the walls of the zeolite structure are rather unlikely.

Region 3000–2400 cm^{-1} . According to literature data, in this region we can find IR bands corresponding to $(\text{O}-\text{H}\cdots\text{N})$ and $(\text{N}-\text{H}^+\cdots\text{O})$ bonds.²⁹

The $\nu(\text{O}-\text{H}\cdots\text{N})$ vibration corresponds to acidic hydroxyls (stronger than silanols) interacting by hydrogen bonding with the probe molecule. A rather broad band is expected in this region for this type of interaction.

The $\nu(\text{N}-\text{H}^+\cdots\text{O})$ vibration corresponds to TMAH^+ formation. In this case, the $\nu(\text{OH})$ band disappears as the proton transfer occurs and a new well-defined band typical of the N-H bond is detected. The wavenumber of this new band may be more or less shifted according to the perturbation induced by the basic zeolitic oxygens and/or neighboring TMA molecules. Thus, a higher wavenumber corresponds to a more acidic Brønsted site (less perturbed by the basic zeolitic oxygen and/or additional TMA molecule), whereas a lower wavenumber indicates an important perturbation by neighboring bases. From the previously described theoretical study,²⁶ the $\nu(\text{N}-\text{H})$ of free trimethylammonium ion should appear around 2821 cm^{-1}

TABLE 1: Literature Data^a

$\delta(\text{CH}_3)$ liquid ²⁵	$\delta(\text{CH}_3)$ TMA–BF ₃ complex ²⁵	$\delta(\text{CH}_3)$ TMA–HCl complex ³¹	$\delta(\text{CH}_3)$ (TMAH) ₂ SiF ₆ ²³
1465 (asym A ₁) 1437 (asym E)	1507 (Sh), 1487–1470 (Sh), 1467–1457 (asym)	1473–1469 (asym A ₁) 1454–1440 (asym E)	1470 (asym)
1380 (sym E)	1413–1380 (sym)	1405 (sym E)	1415–1400 (sym)

^a Sh: Shoulder. asym and sym: asymmetric and symmetric deformation modes (with A₁ and E being the overall vibrational symmetry reported when available).

(protonated species, unperturbed by the oxygens). Therefore, studying this region one can obtain information about the type of formed species (protonated or hydrogen bonded) and the relative acid strength of the involved hydroxyls groups.

As previously explained, according to the zeolite and probe molecule sizes,^{20,21} TMA can access the whole cavities of the ZSM-5 structure. Moreover, the possible heterogeneity of hydroxyls groups is not detected in our H–ZSM-5 sample (Si/Al = 29).²² We thus propose that only one type of protonated species is formed. This idea is confirmed by the appearance of a typical $\nu(\text{N–H})$ well-defined band at 2760 cm^{−1} (Figure 1) and its constant position as long as increasing quantities of TMA are added. This observation is consistent with the appearance of bands at 3053 and 3018 cm^{−1} indicating transfer of the nitrogen lone pair to a proton as extensively described before. Furthermore, disappearance of the $\nu(\text{N–H})$ band at 2760 cm^{−1} during TPD only occurred at temperatures above 623 K, while acidic hydroxyls at 3610 cm^{−1} started to be restored. This is consistent with a strongly adsorbed TMAH⁺ species. We will see later how the position of the $\nu(\text{N–H})$ wavenumber can provide a measure of the acidic strength.

Associated to the band at 2760 cm^{−1} one can observe two small bands at 2530 and 2488 cm^{−1} which both disappear during TPD experiments. These bands should be related to methyl group deformation modes (overtone or combinations) because their position remains constant when TMA adsorption is carried out in other compounds with very different acidic strengths (as shown later).

Region 1600–1350 cm^{−1}. Concerning the bending region, a parallel shift of the stretching $\nu(\text{CH})$ and bending $\delta(\text{CH}_3)$ bands was already observed.²⁴ Thus, we expect a shift to higher wavenumber for the $\delta(\text{CH}_3)$ bands when the interaction strength between the N atom of trimethylamine and the zeolitic proton increases. Some bibliographic data are reported in Table 1 in which some band splittings are observed. According to Wang et al.,³⁰ CH₃ bending is very sensitive to intermolecular interactions and is often used to indicate the packing state of a hydrocarbon chain. Thus, the appearance of several bands in the TMA complex (well-defined structure) may be due to intermolecular interactions.

For the TMA increasing amounts (to 980 mol g^{−1}) adsorption in our H–ZSM-5 zeolite (Figure 1), four bands can be distinguished in the bending region at 1485, 1475, 1455, and 1420 cm^{−1}. Docquir et al.,³² studying methylamine adsorption in a series of zeolites, assigned bands at 1481, 1465, and 1427 cm^{−1} to $\delta(\text{H–C–H})$ vibration modes of adsorbed methylamine in a NaBeta zeolite. According to these authors, we propose that our triplet at 1485, 1455, and 1420 cm^{−1} corresponds to $\delta(\text{H–C–H})$ deformation modes of TMA strongly interacting inside the zeolite micropores (TMAH⁺ species). For a 133 Pa TMA equilibrium pressure, it was observed (upper spectrum on Figure 1) that the 1475 cm^{−1} band is the most intense $\delta(\text{H–C–H})$ component of TMA weakly interacting with silanols by H bonding. The four distinct $\delta(\text{H–C–H})$ vibration modes observed in our case thus result from TMA interacting both

strongly with SiOHAl (the main species while increasing TMA amounts) and slightly with SiOH. A Davydov-type band splitting induced by dynamic coupling between neighboring TMAH⁺ could be another explanation. Concerning the $\delta(\text{NH}^+\cdots\text{O})$ vibration, it was observed in previous studies around 1215 cm^{−1} in the [(CH₃)₃NH]₂SiF₆ ionic salt²³ or in the range 1310–1365 cm^{−1} in acidic liquid solution²⁹ and thus is not observed in H–ZSM-5 because of the framework SiOAl strongly absorbing IR vibrations.

Thus far, we defined the three more important regions in the spectra of TMA adsorbed on a homogeneously acidic H–ZSM-5 sample. We confidently assigned the observed bands to the corresponding vibration modes and from this knowledge we can undertake the TMA adsorption in the more complex HY sample.

TMA Adsorption on the Y Zeolite. The appearance of at least two distinct species after TMA adsorption in our HY zeolite is expected since at least two different accessible hydroxyls are present in such compound. The spectra recorded before and after TMA saturation (133 Pa of TMA at equilibrium) at room temperature are shown in Figure 2.

After saturation only one remaining band is detected at 3501 cm^{−1} in the $\nu(\text{OH})$ region. According to a previous work,¹⁷ this very low wavenumber $\nu(\text{OH})$ band corresponds to hydroxyl groups located in the hexagonal prisms which are inaccessible to this big probe molecule. Interaction of TMA molecule with hydroxyls groups located in large cavities (3638 cm^{−1}) and sodalite units (~3550 cm^{−1}) is evident. Nevertheless, it is not possible for TMA to enter inside the sodalite units¹⁸ (due to its steric hindrance: diameter of sodalite aperture is ~2 Å³³ and size of TMA ≈ 5.24 Å); thus, a rather “long distance” interaction with these hydroxyls is expected. Effectively, as it is a strong basic molecule, TMA can perturb hydroxyls inside sodalite units by hydrogen bonding (high bond length). The complexity of the obtained spectrum, especially the broad band around 2400 cm^{−1} (which was absent for the previous H–ZSM-5 sample) is consistent with this statement as it could correspond to the $\nu(\text{O–H}\cdots\text{N})$ vibration. A good candidate for the corresponding $\delta(\text{O–H}\cdots\text{N})$ vibration is the rather wide component at 1380 cm^{−1} (also absent for our H–ZSM-5 sample), but this will be discussed later. Compared with the H–ZSM-5 results, we assign the band at 2650 cm^{−1} to the $\nu(\text{N–H})$ vibration of protonated species.

Room-Temperature Adsorption of TMA Increasing Amounts on HY. To obtain further information about the different interactions occurring between TMA and acidic hydroxyls in the HY structure, we studied the evolution of the surface during the adsorption at room temperature of increasing amounts of TMA. The corresponding spectra are presented on Figure 3.

First, it is important to notice that $\nu(\text{OH})$ at 3638 cm^{−1} (supercage hydroxyls) and $\nu(\text{OH})$ at 3550 cm^{−1} (sodalite hydroxyls) always disappear together, i.e., whatever the TMA amount. Jointly, both the $\nu(\text{CH})$ vibration at $\bar{\nu} > 3000$ cm^{−1} (doublet at 3035 and 3004 cm^{−1}, typical of TMAH⁺) and $\nu(\text{CH})$ at 2944 cm^{−1} (typical of weak interaction) appear together. This means that in the absence of heating, both TMA protonation

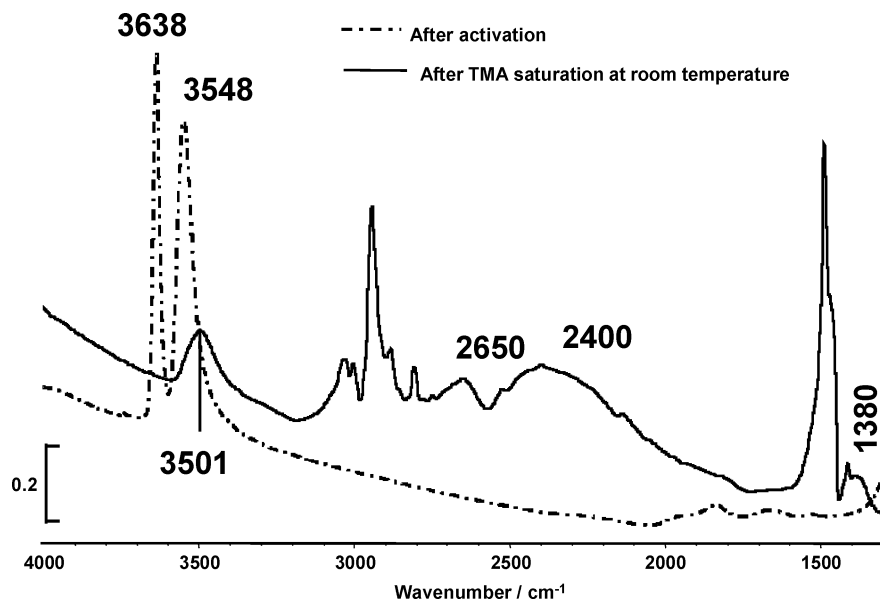


Figure 2. Spectrum of HY before and after saturation with TMA (133 Pa at equilibrium) at room temperature.

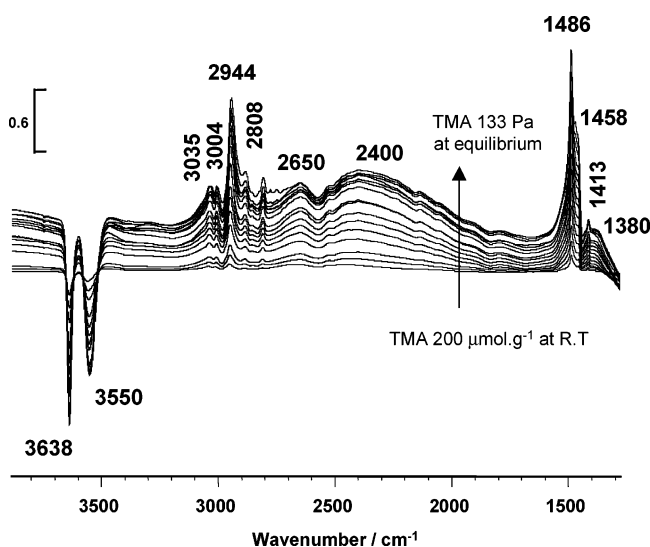


Figure 3. Spectra after increasing amount of TMA adsorbed over HY at room temperature. Spectrum of HY before TMA adsorption was subtracted shown for clarity.

and interaction via hydrogen bonding take place simultaneously. Contrary to what was observed with the H-ZSM-5 sample, the intensity of the $\nu(\text{CH})$ component below 3000 cm^{-1} (at 2944 cm^{-1}) is rather high and its relative intensity compared with that of the doublet at $\bar{\nu} > 3000\text{ cm}^{-1}$ is kept high whatever the coverage level. Even if the respective $\nu(\text{CH})$ molar extinction coefficients are not known, the differences observed between H-ZSM-5 and HY zeolites are consistent with a greater number of interactions by hydrogen bonding inside the HY structure. Moreover, as the molar extinction coefficients $\epsilon(\text{OH}_{\text{H.F}})$ for the supercage hydroxyls at 3638 cm^{-1} (mainly responsible for TMAH^+) are higher than the $\epsilon(\text{OH}_{\text{L.F}})^{34}$ for the smaller cavity hydroxyls at 3550 cm^{-1} (mainly responsible for H-bonded TMA), comparison of the relative intensities of the negative $\nu(\text{OH})$ bands allows us to assume that the amount of formed TMAH^+ and hydrogen-bonded TMA species are about the same.

Focusing on the $1600\text{--}1350\text{ cm}^{-1}$ region, we mainly observe three fine peaks at 1486 , 1458 , and 1413 cm^{-1} whose intensities increase together with the TMA amount. In agreement with the previous experiment with H-ZSM-5 and according to literature data, we attribute these vibrations to $\delta(\text{CH})$ modes. For the

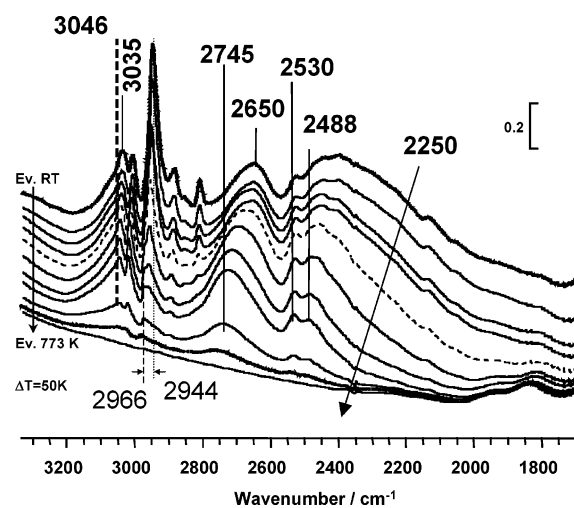


Figure 4. IR spectra during thermo-programmed desorption experiments in HY zeolite.

highest TMA amounts, one more $\delta(\text{CH})$ band appears at 1470 cm^{-1} (not indicated on the figure for clarity) which is due to very little interacting (pseudo-liquid like) TMA species.

Finally, the broad bands at 2650 , 2400 , and 1380 cm^{-1} also increase together. It is thus difficult, when adsorbing TMA at room temperature, to selectively probe only one type of site and precisely identify the nature of the various interactions. For this purpose, we studied the thermal stability of the adsorbed species.

TMA Desorption at Increasing Temperature. Evolution of the spectra as a function of the evacuation temperature (Figure 4) shows the first disappearance (for the lower temperature) of the broad band in the $2400\text{--}2000\text{ cm}^{-1}$ region, which should correspond to hydrogen-bonded species (medium-strong interaction according to Novak³⁵). Simultaneous with the broad feature, the low-wavenumber $\nu(\text{CH})$ band at 2944 cm^{-1} (close to liquid TMA) disappears, revealing its characteristics of methyl groups stretching modes of H-bonded TMA. The correlation between the disappearance of these bands and the re-appearance of the low-wavenumber hydroxyls (373 and 423 K) is evident from the successive difference spectra (Figure 5). These results confirm that the hydroxyls located in the sodalite units (at least a majority of them) interact with the TMA molecule by

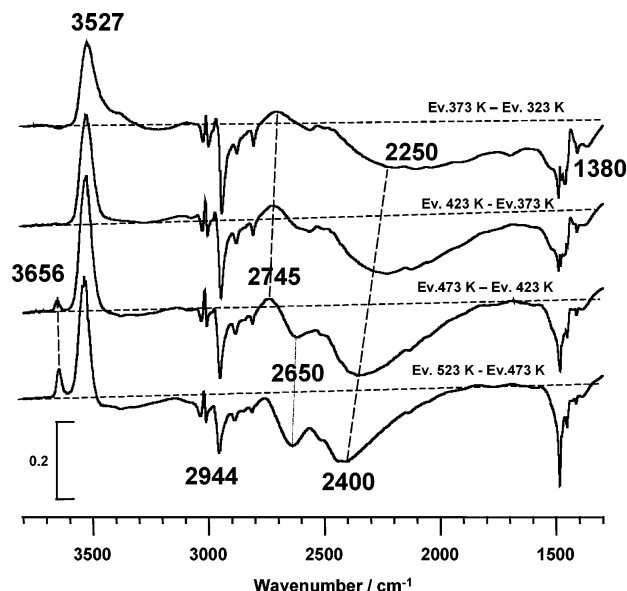


Figure 5. Spectra resulting from subtraction between spectra obtained for two consecutive evacuation temperatures during TPD experiments in HY.

hydrogen bonding. Note that the $\nu(\text{OH})$ wavenumber typical of restored sodalite hydroxyls in the presence of TMAH^+ inside the supercages (3527 cm^{-1}) is different from the $\nu(\text{OH})$ wavenumber typical of free sodalite hydroxyls (3550 cm^{-1}).

For higher desorption temperature (starting from 473 K, dashed spectrum on Figure 4), the ratio between the intensity of the TMAH^+ $\nu(\text{CH})$ doublet (at $3035 \rightarrow 3046$ and 3004 cm^{-1}) and the H-bonded TMA $\nu(\text{CH})$ at 2944 cm^{-1} band starts to be reversed (i.e., to be higher than one), which means that TMAH^+ are the main remaining species above 473 K. At this temperature we also clearly distinguish the doublet at $2530\text{--}2488\text{ cm}^{-1}$, which was already observed for the H–ZSM-5 sample and attributed to methyl group vibration modes (overtone or combinations). When the temperature reaches 673 K, only one well-defined band centered around 2745 cm^{-1} remains in the $\nu(\text{NH})$ region and the corresponding $\nu(\text{CH})$ peak is centered at 3046 cm^{-1} . This traduces a very stable TMAH^+ species (trimethylammonium), indicating the presence of a strongly acidic Brønsted site. Considering the spectra in Figure 4, it seems that both $\nu(\text{NH})$ and $\nu(\text{CH})$ vibrations not only decrease but shift with the evacuation temperature as well.

To clarify what happens during desorption, we present in Figure 5 the spectra corresponding to what is observed between two consecutive evacuation temperatures. The dotted straight line represents for each spectrum the “zero level” corrected from baseline deviation: bands above the dotted line appear whereas bands beneath the dotted line disappear during evacuation. The upper spectrum thus indicates that hydroxyls at 3527 cm^{-1} are restored when increasing the evacuation temperature from 323 to 373 K. At the same time, the $\nu(\text{CH})$ band at 2944 cm^{-1} , the $\delta(\text{CH})$ massif, and the broad bands at 2250 and 1380 cm^{-1} disappear, traducing the loss of hydrogen-bonded species. In the $\bar{\nu} > 3000\text{ cm}^{-1}$ zone, we observe both positive and negative $\nu(\text{CH})$ peaks which indicate perturbation of protonated species while desorbing H-bonded TMA. This fact is clearly confirmed in the $\nu(\text{NH})$ region where a positive $\nu(\text{NH})$ band continuously appears till 473 K. At this temperature, this new $\nu(\text{NH})$ band is centered at 2745 cm^{-1} .

The occurrence of TMA protonation for low desorption temperature is meaningless: in fact, the new $\nu(\text{NH})$ component is always associated with a corresponding negative $\nu(\text{NH})$ one

at lower wavenumber. As an explanation we propose that during the desorption of TMA H bonded with sodalite hydroxyls (restoration of $\nu(\text{OH})$ at 3527 cm^{-1} typical of sodalite hydroxyls in the presence of TMAH^+ in the supercages) the TMAH^+ formed in the supercages interacts less and less with basic surrounding entities (both zeolitic oxygens and neighboring H-bonded TMA), thus leading to more and more “free” TMAH^+ molecules with higher associated $\nu(\text{NH})$. This phenomenon takes place from 323 to 473 K. As a primary conclusion, we report that this temperature range corresponds to elimination of H-bonded TMA mainly characterized by the following negative bands: $\nu(\text{CH})$ at 2944 cm^{-1} , broad $\nu(\text{OH}\cdots\text{N})$ at $2250\text{--}2400\text{ cm}^{-1}$, and tentatively assigned $\delta(\text{OH}\cdots\text{N})$ at 1380 cm^{-1} . Starting from 473 K, the recovery of a small amount of high-wavenumber hydroxyls at 3656 cm^{-1} is detected, while the intensity of the 2650 cm^{-1} $\nu(\text{N}\text{--}\text{H})$ vibration decreases without (or very little) associated $\nu(\text{NH})$ at higher wavenumber: protonated species are no longer perturbed but start to decompose. This fact is confirmed during the evacuation between 473 and 523 K (lower spectrum) for which no positive bands other than hydroxyls are observed. Nevertheless, we must emphasize that in this last temperature range both H-bonded TMA (negative bands at 2944 and 2400 cm^{-1}) and TMAH^+ (negative doublet at $\nu > 3000\text{ cm}^{-1}$ and negative band at 2650 cm^{-1}) are removed. Focusing on the $1600\text{--}1350\text{ cm}^{-1}$ region, it seems that the 1380 cm^{-1} band evolution is correlated with the 2944 cm^{-1} one, which would confirm its assignment to the bending mode of hydroxyls in hydrogen bonding with TMA. For higher evacuation temperatures, the spectra are even more complex (not shown), but we observe that the supercages hydroxyls characterized by a $\nu(\text{OH})$ at 3638 cm^{-1} are restored while the TMAH^+ species with $\nu(\text{NH})$ at 2745 cm^{-1} are eliminated.

Finally, we can conclude that TMA adsorption at room temperature leads to various interactions depending on both the nature of the involved acidic hydroxyls and the TMA concentration inside the micropores. (i) On one hand, interaction with sodalite hydroxyls takes place via “long-range” hydrogen bonding since the TMA molecules remain in the supercages. A rough estimation of the $\text{R}(\text{O}\cdots\text{N})$ distance between O and N atoms in the $[\text{ZO}\text{--}\text{H}\cdots\text{N}]$ complex can be determined from Novak’s curves,³⁵ which were reported for H-bonded complex implying two basic oxygen atoms. We estimated in our case the $\text{R}(\text{O}\cdots\text{N})$ value to be 2.6 \AA , which is low enough to characterize a rather strong H bond. Nevertheless, applying the empirical relation $\Delta\nu(\text{OH})/\nu(\text{OH}) = 3.6\Delta r(\text{OH})$, where $\Delta\nu(\text{OH})$ is the $\nu(\text{OH})$ shift upon H bonding as compared to the free $\nu(\text{OH})$ vibration and $\Delta r(\text{OH})$ is O–H bond elongation upon H bonding,³⁵ we find $\Delta r(\text{OH}) = (3527 - 2250)/3527 \cdot 3.6 = 0.10\text{ \AA}$. Taking into account that the O_2H average bond length for hydroxyls located inside supercages is $1.02(5)\text{ \AA}$ as calculated from neutron diffraction data,³⁶ we conclude that the O_2H bond length is increased by around 10%, the proton remaining however closer to its framework basic oxygen than to the TMA basic nitrogen. This conclusion is consistent with the impossibility for the bulky TMA to enter the sodalite units. (ii) On the other hand, proton transfer from the hydroxyls located inside the supercages occurs to yield TMAH^+ . A part of the formed TMAH^+ characterized by a $\nu(\text{NH})$ at 2650 cm^{-1} is decomposed under evacuation temperature starting from 473 K to restore free hydroxyls at 3656 cm^{-1} . Another part of TMAH^+ is perturbed by the basic surrounding entities (both zeolitic oxygens and neighboring H-bonded TMA). This perturbation was evidenced during desorption at low temperatures for which proton transfer to TMA was enhanced to

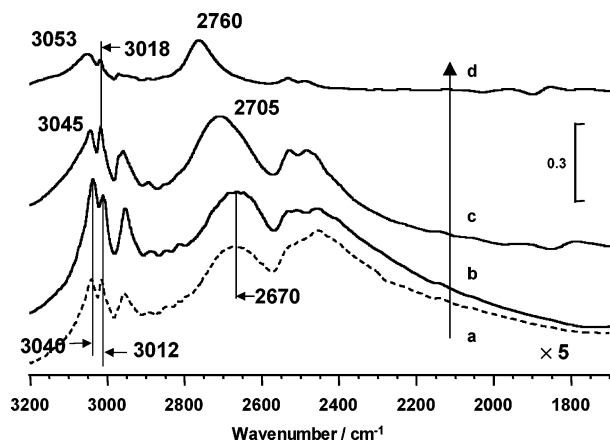


Figure 6. Spectra of (a) HNaX10, (b) HNaX40, (c) HY, and (d) H-ZSM-5 after TMA adsorption and evacuation at 523 K. The spectrum of HNaX10 was multiplied by a factor 5 in order to obtain a comparable scale.

generate more “free” TMAH⁺ molecules characterized by a $\nu(\text{NH})$ at 2745 cm⁻¹. The so-formed “free” TMAH⁺ are very stable and only completely decomposed at temperatures as high as 773 K to restore free hydroxyls at 3638 cm⁻¹. In our opinion, the two distinct $\nu(\text{N-H})$ bands observed during TMA desorption associated with recovery of hydroxyls at 3656 and 3638 cm⁻¹ reveal the presence of at least two distinct acidic strengths for the hydroxyls located inside the supercages. For the same site location, the local chemical factor should then play a role: the aluminum distribution in the framework is not necessarily homogeneous, and the number of Al next-nearest neighbors influences the acidic strength of a given site. Another explanation for the 3656 cm⁻¹ unusual component could be that part of the O₄ crystallographic sites is a proton holder³⁷ for this low Si/Al ratio HY sample.

Use of TMA for Characterization of Acidic Strength. In a previous part of this paper we gave evidence that TMA could be protonated in zeolite micropores of ZSM-5 and Y-FAU types. The proton transfer leads to a N-H bond formation characterized by an IR-active $\nu(\text{NH})$ vibration. The so-formed TMAH⁺ cation may however remain in interaction with the framework basic oxygens and/or neighboring basic molecules. The stronger these perturbations of TMAH⁺, the weaker the N-H bond and thus the lower the associated $\nu(\text{NH})$ wavenumber. With the aim of probing the intrinsic acidic strength of zeolitic hydroxyls we then must get rid of neighboring TMA molecules in order to only keep the effect of the surrounding framework oxygens (which are the bases associated with the probed acidic hydroxyls). For this purpose, we propose to evacuate TMA under a vacuum at 523 K. Effectively, we demonstrated that this is the required temperature to remove H-bonded TMA-perturbing TMAH⁺ in supercages.

To validate our method, we decided to extend the study of TMA adsorption to NaHX samples, which are known to possess weaker acidic sites.⁵ These NaHX zeolites were obtained by ionic exchange starting from the sodium form: $\text{Na}^+ \leftrightarrow \text{NH}_4^+$. The exchange degrees were 40% and 10%, respectively, for NaHX40 and NaHX10, and it may be supposed that after evacuation of TMA at 523 K mainly TMAH⁺ ions remain in the supercages of the X-FAU structure. Considering only the average chemical factor of our samples, the following acidic strength ranking is expected: H-ZSM-5 > HY > NaHX10 \approx NaHX40. The spectra obtained after adsorption of TMA followed by evacuation at 523 K for our four zeolites (H-ZSM-5, HY, NaHX40, and NaHX10) are shown in Figure 6. At such

an evacuation temperature all samples have spectra with about the same intensity ratio $\nu(\text{CH}) > 3000 \text{ cm}^{-1} / \nu(\text{CH}) < 3000 \text{ cm}^{-1} > 1$, which confirms that for all samples TMAH⁺ is the main remaining species.

As discussed previously, formation of an interaction involving a transfer of the nitrogen lone pair (total or partial) increases the wavenumber of $\nu_{\text{as}}(\text{C-H})$ bands and the shift magnitude is a function of the interaction strength. From Figure 6 we report $\nu(\text{CH})$ at 3053 cm⁻¹ for H-ZSM-5 > $\nu(\text{CH})$ at 3045 cm⁻¹ for HY > $\nu(\text{CH})$ at 3040 cm⁻¹ for both NaHX samples, which is in perfect agreement with the previously proposed acidic strength ranking. Considering the $\nu(\text{NH})$ vibrations, we also report $\nu(\text{NH})$ at 2760 cm⁻¹ for H-ZSM-5 > $\nu(\text{NH})$ at 2705 cm⁻¹ for HY > $\nu(\text{NH})$ at 2670 cm⁻¹ for both NaHX samples. The $\nu(\text{NH})$ vibration of TMAH⁺ is thus a good indicator of acidic strength and much more sensitive [$\Delta\nu(\text{NH}) = 2760 - 2670 = 90 \text{ cm}^{-1}$] than the $\nu_{\text{as}}(\text{CH})$ one [$\Delta\nu_{\text{as}}(\text{CH}) = 3053 - 3040 = 13 \text{ cm}^{-1}$]. Note that the $\nu(\text{NH})$ at 2705 cm⁻¹ for HY is still after evacuation at 523 K a composite band made of 2745 and 2650 cm⁻¹ components which traduces the heterogeneity of supercages hydroxyls. Furthermore, the two X-FAU samples where only Na amount differs give the same TMAH⁺ spectra. This means that no effect of the Na content on the acidic strength is detected for our NaHX samples by this method.

Adsorption of TMA yielding TMAH⁺, whose typical vibrations are acidic strength sensitive, appears to be an interesting complementary tool for elaboration of a surface acidity scale, provided that evacuation of neighboring TMA molecules is carefully performed.

Conclusions

TMA as a probe for acidity investigation on zeolitic compounds by IR spectroscopy has been studied in depth for the first time. Identification of the typical bands of protonated species and hydrogen-bonded species formed after TMA interaction with the acid sites of a HY zeolite was made on the basis of bibliographic and experimental data (previous TMA adsorption in H-ZSM-5). From thermo-programmed desorption experiments we can affirm TMAH⁺ species are formed from the supercage hydroxyls while hydrogen-bonded species are produced by interaction with the less accessible hydroxyl groups (sodalite units) showing a typical $\nu(\text{OH} \cdots \text{N})$ broad band in the 2400–2000 cm⁻¹ region with associated $\delta(\text{OH} \cdots \text{N})$ around 1380 cm⁻¹.

Considering the TMAH⁺ species, we observed that part of them was perturbed by the presence of neighboring TMA H bonded with sodalite hydroxyls. Evacuation of these H-bonded species at rather low temperature (to 523 K) leads to “free TMAH⁺”, which are only decomposed at high temperature (773 K) to restore the strongly acidic hydroxyls at 3638 cm⁻¹. Another part of TMAH⁺ species is less sensitive to the presence of H-bonded TMA and less stable as its decomposition starts from evacuation at 523 K. The associated hydroxyls at 3656 cm⁻¹ are proposed to be located inside the supercages and have a lower acidity than the 3638 cm⁻¹ ones. At least two types of acid sites would then be located in the large cavities of a HY zeolite: both different local chemical factors and different crystallographic positions are suggested to explain this multiplicity of supercage hydroxyls.

Finally, we affirm that the positions of typical bands of TMAH⁺ are very sensitive to the acidic strength of the surface: thus, it seems possible to use this probe molecule to compare the Brønsted acidity of different zeolites (with no steric hindrance).

References and Notes

- (1) Stöcker, M. *Microporous Mesoporous Mater.* **2005**, 82 (3), 257.
- (2) Venuto, P.; Landis, P. *Adv. Catal.* **1968**, 18, 259.
- (3) Datka, J.; Boczar, M.; Gil, B. *Colloids Surf., A* **1995**, 105, 1.
- (4) Pais da Silva, M. I.; Lins da Silva, F.; Tellez, S. C. A. *Spectrochim. Acta, Part A* **2002**, 58, 3159.
- (5) Oliviero, L.; Vimont, A.; Lavalley, J. C.; Romero Sarria, F.; Gaillard, M.; Maugé, F. *Phys. Chem. Chem. Phys.* **2005**, 7, 1861.
- (6) Maache, M.; Janin, A.; Lavalley, J. C.; Benazzi, E. *Zeolites* **1995**, 15, 507.
- (7) Tonetto, G.; Atias, J.; de Lasa, H. *Appl. Catal., A* **2004**, 270, 9.
- (8) Lonyi, F.; Valyon, J. *Thermochim. Acta* **2001**, 373, 53.
- (9) Lonyi, F.; Valyon, J. *Microporous Mesoporous Mater.* **2001**, 47, 293.
- (10) Choudhary, V. R.; Akolekar, D. B. *J. Catal.* **1989**, 119, 525.
- (11) Lavalley, J. C.; Anquetil, R.; Czyzniewska, J.; Ziolk, M. *J. Chem. Soc., Faraday Trans.* **1996**, 92, 1263.
- (12) Knoezinger, H.; Huber, S. *J. Chem. Soc., Faraday Trans.* **1998**, 94, 2047.
- (13) Cairen, O.; Chevreau, T. *J. Chem. Soc., Faraday Trans.* **1998**, 94, 323.
- (14) Zecchina, A.; Marchese, L.; Bordiga, S.; Paze, C.; Gianotti, E. *J. Phys. Chem. B* **1997**, 101 (48), 10128.
- (15) Bevilacqua, M.; Busca, G. *Catal. Commun.* **2002**, 3, 497.
- (16) Corma, A.; Fornés, V.; Forni, L.; Marquez, F.; Martinez-Triguero, J.; Moscotti, D. *J. Catal.* **1998**, 179, 451.
- (17) Romero, S. F.; Marie, O.; Saussey, J.; Daturi, M. *J. Phys. Chem. B* **2005**, 109 (5), 1660.
- (18) Earl, W. L.; Fritz, P. O.; Gibson, A. A. V.; Lunsford, J. H. *J. Phys. Chem.* **1987**, 91, 2091.
- (19) Payen, E.; Grimblot, J.; Lavalley, J. C.; Daturi, M.; Maugé, F. Application of Vibrational Spectroscopy in the Characterization of Oxides and Sulfides Catalysts. *Handbook of Vibrational Spectroscopy*; Chalmers, J. M., Griffith, P. R., Eds.; Wiley: New York, 2002; Vol. 4.
- (20) Olson, D. H.; Kokotailo, G. T.; Lawton, S. L.; Meier, W. M. *J. Phys. Chem.* **1981**, 85, 2238.
- (21) Bondi, A. *J. Phys. Chem.* **1964**, 68, 441.
- (22) Datka, J.; Gil, B.; Baran, P. *Microporous Mesoporous Mater.* **2003**, 58, 291.
- (23) Ouasri, A.; Rhandour, A.; Dhamelincourt, M. C.; Dhamelincourt, P.; Mazzah, A. *Spectrochim. Acta, Part A* **2003**, 59, 851.
- (24) Harmon, K. M.; Gennick, I.; Madeira, S. L. *J. Phys. Chem.* **1974**, 78 (25), 2585.
- (25) Taillandier, E. Ph.D. Thesis, Paris, 1970.
- (26) Jiang, N.; Yuan, S.; Wang, J.; Jiao, H.; Qin, Z.; Li, Y.-W. *J. Mol. Catal. A: Chem.* **2004**, 220, 221.
- (27) Schleyer, P. v. R.; Kos, A. *J. Tetrahedron* **1983**, 39, 1141.
- (28) Mui, C.; Han, J. H.; Wang, G. T.; Musgrave, C. B.; Bent, S. F. *J. Am. Chem. Soc.* **2002**, 124, 4027.
- (29) Wierzejewska, M.; Ratajczak, H. *J. Mol. Struct.* **1997**, 416, 121.
- (30) Wang, W.; Gu, B.; Liang, L.; Hamilton, W. *J. Phys. Chem. B* **2004**, 108, 17477.
- (31) Barnes, A. J.; Nicholas, J.; Kuzniarski, S.; Mielke, Z., *J. Chem. Soc., Faraday Trans. 2* **1984**, 4, 465.
- (32) Docquir, F.; Norberg, V.; Toufar, H.; Paillaud, J. L.; Su, B. L. *Langmuir* **2002**, 18, 5963.
- (33) Breck, D. W. *J. Chem. Educ.* **1964**, 41 (12), 678.
- (34) Thibault-Starzyk, F.; Gil, B.; Aiello, S.; Chevreau, T.; Gilson, J. P. *Microporous Mesoporous Mater.* **2004**, 67, 107.
- (35) Novak, A. *Struct. Bonding* **1974**, 18, 177.
- (36) Czjzek, M.; Jobic, H.; Fitch, A. N.; Vogt, T. *J. Phys. Chem.* **1992**, 96, 1535.
- (37) Mortier, W. J.; Pluth, J. J.; Smith, J. V. *J. Catal.* **1976**, 45, 367.